Journal of Materials and Manufacturing (2023) 2: 10-19

Journal of Materials and Manufacturing

A study of erosion wear behavior of Inconel-718 nickel-based superalloy at different impingement angles

Mustafa Kaplan*

Bilecik Şeyh Edebali University, Vocational School, Department of Machinery and Metal Technologies, Metallurgy Program, 11100 Bilecik, Turkey
(ORCID: 0000-0002-6662-2051), mkaplan5442@gmail.com

Abstract

Inconel-718 Nickel Based Superalloy used especially in aerospace applications materials are subject to solid particle erosion. Solid particle erosion causes the structural integrity of Inconel 718 materials to deteriorate. Therefore, it reduces the service life of the material. In this study, it is aimed to investigate the variation of Inconel-718 solid particle erosion resistance depending on the particle impingement angle. The erosion testing was carried out using air-jet erosion test rig (ASTM G76-13) 30°,60° and 90° impingement angle. After the erosive wear tests, the eroded surfaces were examined with a three-dimensional (3D) optical surface profilometer. In order to provide the erosive wear distribution of Inconel 718, the proportions of the sections of the samples, the areal surface roughness values, the 3D surface topographies and the surface morphology were examined according to the surface impact properties. In conclusion, the maximum wear occurred at the impingement angle of 30°, which is an indication of ductile impressions. In addition, the surface roughness values and surface topographies have also changed significantly depending on the impact angle. It has deeper and wider craters at an impact angle of 30° and its craters are visualized by profilometry analysis.

Keywords: Inconel 718; Solid particle erosion; Impingement angles; Erosion mechanisms.

Nomenclature	
3D	Three-Dimensional
Ra	Surface roughness
Sa	Average roughness of surface area
Sv	Maximum pit depth of surface area
Sp	Maximum roughness of surface area
m1	The mass of the sample before erosion
m2	The mass of the sample after erosion
ṁ	Mass flow rate of erodent particles
Δm	Mass loss of sample (mg)
E	Erosion rate

1. Introduction

Superalloy materials are used in many fields, especially in the aerospace and defense industries. Superalloys are materials developed for applications where high mechanical stresses occur [1,2]. It can also be defined as

* Corresponding author
E-mail addresses: mkaplan5442@gmail.com
DOI: 10.5281/zenodo.10014151
Received: 25 August 2023 / Accepted: 1 October 2023
ISSN: 2822-6054 All rights reserved.

alloys that contain elements such as titanium, nickel, niobium, cobalt and iron, which maintain their stability against high stresses and temperatures in harsh environmental conditions. Superalloy materials have very high hardness values [3]. Another important feature is their high resistance to hot corrosion and abrasion for a long time at high temperatures such as 650 °C. Superalloy materials are grouped into three groups: nickel, chromium, cobalt and iron-based alloys, cobalt-based and nickel-based alloys formed by carbide strengthening and solid precipitation hardening. The alloys are common materials and alloys used in aircraft engine production. The materials are expected to withstand aggressive operating environments such as solid particle erosion, high temperature resistance and high temperature corrosion [3,4]. Nickel-based alloys are the most widely used superalloys, accounting for 50% by weight of the alloys used in aircraft engines, primarily in gas turbine compartments. Nickel alloys provide a higher strength-to-weight ratio compared to the denser steels. The use of nickel-based alloys in such aggressive environments depends on their high corrosion resistance, mechanical and thermal fatigue, creep and erosion resistance at high temperatures. In areas where nickel-based alloys are used, these properties are essential for effective operational performance. In aircraft engines, the need for these properties is particularly evident in turbine blades used under high pressure and temperature [5-8]. Inconel 718 is a nickel - chromium superalloy with high strength, corrosion resistance. Inconel 718 has good tensile, fatigue, creep and rupture strain. It is therefore used in a wide range of applications. Because these parts require high temperature strain and high corrosion resistance. Inconel 718 is used in the aerospace industry is a commercial superalloy [9,10].

Erosive wear can be defined as an important problem in many industrial components, especially in jet turbines and steam systems. Hard atmospheric conditions such as dust storms, volcanic ash and ice particles can cause corrosion and deterioration of aviation components. Engineering materials are exposed to many harmful external influences in an abrasive environment during service operation. Erosive wear occurs as a result of the fact that the working environment contains solid particles and under severe working conditions, solid particles repeatedly hit the material surface at high speeds and at different angles. Solid particle erosion in a nutshell is defined as the removal of material from the surface [11-14]. The main purpose of this paper is to reveal the erosion behavior of Inconel 718 superalloy impingement different impingement angles. The surface topography and the morphology of eroded of the Inconel 718 were investigated based on the impingement angle of the particles to highlight the solid particle erosion behavior.

2. Material and Method

2.1. Preparation of Superalloy Material

In this study, Inconel 718 nickel-based superalloy material was used. The samples used were prepared in the form of 1 inch and 4 mm discs, see Fig.1. Inconel 718 superalloy used in the tests. The chemical composition of Inconel 718 superalloy is given in Table 1.

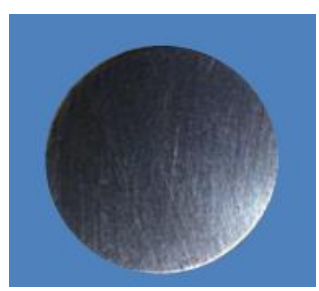

Fig. 1. Inconel 718 superalloy used in the tests

Table 1. Chemical composition for Inconel-718 (% weight)

Elements	Ni	Cr	Nb	Ti	Co	Mo	Al	Cu	C	Fe
Wt.%	53	19	5.1	0.9	0.9	3.1	0.5	0.15	0.08	Bal.

2.2. Metod

This paper is focused on investigating the solid particle erosion behavior of nickel-based Inconel 718 Superalloy. The surface roughness values and topography of the eroded area after erosive wear were analyzed with the help of Nanovea PS50 3D optical profilometer. Analyses were performed according to ISO 4287 and ISO 25718 standards. In the examination of the surface roughness values and surface topography of the samples, an area of 5 mm x 5 mm was scanned in the area where erosive wear occurred. After the scanning operations were performed in 15 µm steps, the surface roughness values and surface topographies were analyzed in detail.

2.2.1. Solid particle erosion testing

Air jet erosion test device was used in the tests. The erosive abrasion test setup shown in Figure 2 was designed in accordance with ASTM G76-13 standard. In the literature, abrasive materials such as Alumina, Silicon Carbide and Silica have been used in erosive wear studies [15-17]. In this paper, Alumina abrasive material with a grain size of 180 mesh is selected. Alumina with sharp corners was used in the wear tests as shown in Figure 3.

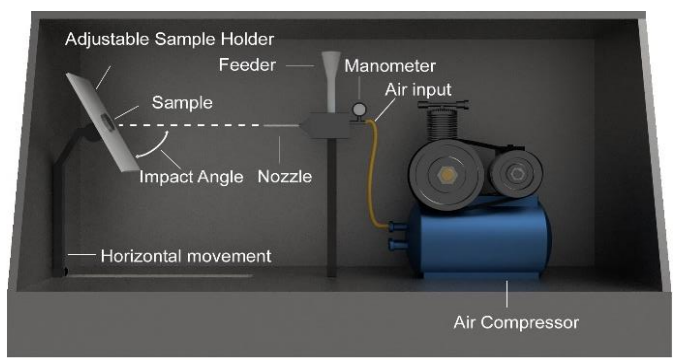

Fig. 2 Solid particle erosion test rig

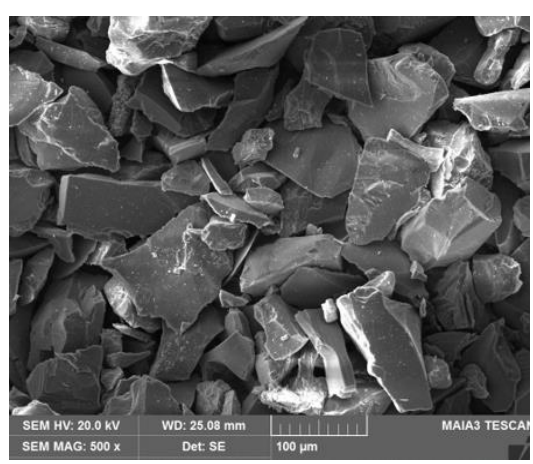

Fig. 3 SEM image of abrasive alumina particles

In the tests carried out at room temperature, the particle impact speed was 27 m/s and the particle impingement angles were 30°, 60° and 90° (Fig.2). In addition, alumina powder with a size of 74-88 μm was exposed to the sample surfaces for 20 seconds. The parameters used in the experiments were determined by considering the studies in the literature and industrial applications (Table 2).

Table 2. Solid particle erosion test parameters

Erodent type	Alumina particles (Al_2O_3)
Erodent size	180 mesh
Particle impingement angle	30°, 60° and 90°
Acceleration/blast gun pressure	1.5 bar
Impingement particle velocity	27 m/s
Mass flow rate	13g/s
Test temperature	25 C^O
Nozzle diameter	5 mm
Nozzle length	50 mm

An analytical balance with a precision of ±0.1 mg was used to determine the weight of the samples before and after the abrasion tests. In calculating the solid particle erosion wear rate, firstly, the sample surfaces were cleaned with compressed air. Then, the pre-wear weights (m_1) of the samples were determined using precision balances. m_2 values were found by measuring the weights of the samples, which were cleaned with compressed air after solid particle erosion and abrasion. Solid particle erosion wear rate was calculated by dividing the difference in sample weights obtained before and after wear by the mass flow rate of the abrasive particle ($\dot{m}$) and time (t). Finally, the erosion rate (E) was calculated according to Equation 1 as follows.

$$E = \frac{(m_1 - m_2)}{\dot{m} \times t} \quad (1)$$

where
E: Erosion rate,
m_1: The mass of the sample before erosion,
m_2: The mass of the sample after erosion,
$\dot{m}$: Mass flow rate of erodent particles,
t: Erosion time.

The erosion rate is defined as the ratio of the mass loss in the eroded sample as a result of solid particle erosion to the total mass of abrasive particles causing this loss. The mass flow rate of abrasive particles varies depending on particle size and spray pressure. In this case, it is obvious that the amount (mass) of particles hitting the samples abraded with particles of different pressures and sizes at the same abrasion time will vary. When it is desired to compare the erosion behavior of the samples eroded with these parameters, it is not a correct method to use the mass loss (Δm) directly in the material. The amount of erosion of materials should be calculated independently of the mass of abrasive particles causing erosion. In summary, when examining the erosion behavior of materials, the amount of erosion per unit abrasive should be calculated. Therefore, the erosion behavior of materials can be compared regardless of the parameters.

2.2.2. Surface roughness and topography analysis

After solid particle erosion experiments, surface roughness and topography examinations of the eroded samples were made with a 3D optic profilometer, Nanovea PS50. Then, effect of the impingement angle of the

fracture on the 3D surface topography and surface roughness of Inconel 718 was investigated by using 3D optical profilometer. The surface roughness variation of the eroded specimens was calculated according to ISO 25178:2-2012.

3. Results and Discussion

3.1. Change in the of erosion rate

Many researchers have studied the effect of impingement angle on wear in solid particle erosion of metallic materials or coatings. In the literature, it has been clearly reported that the particle impingement angle has an important role in the formation of solid particle erosion [19-21].

Inconel 718 is a Nickel-Chromium alloy that can be precipitation hardened. It has a hardness of about 331 Hb and also high creep rupture resistance up to 700 C. Inconel 718 has higher strength than Inconel X750 and has better mechanical properties at low temperatures than Nimonic 90 and Inconel X750. Nickel-based superalloys have a stable microstructure thanks to a high percentage of nickel and their corrosion resistance in reducing (acidic) environments thanks to nickel increases. The addition of chromium gives these alloys hardness, corrosion resistance in oxidizing environments and its resistance to oxidation increases even more. The alloys are characterized by retained strength at high temperatures, good machinability, resistance to corrosion and oxidation they gain a good resistance. Therefore, solid particle erosion resistance is realized in parallel. Especially for long periods above 700 °C high-temperature, as they retain a significant portion of their strength. It is suited to the requirements of their field of application and therefore their field of use is expanding. Depending on the area of use, nickel-based Mo, Co, Nb, Zr, B, Fe and other elements are added to superalloys [22-24].

In brittle materials, maximum material loss occurs at high impact angles. On the other hand, in ductile materials, the maximum material loss occurs at low impact angles (30^{o}). When the variation of material loss with impact time is taken into account, there may be a development phase in ductile materials where the target material weight increases before the wear becomes linearly proportional to time. This period occurs when the abrasive particles are embedded in the ductile target material. Stable erosion behavior is observed after the successive detachment of abrasive particles from the target material surface. Most of the loss in impact energy occurs when roughening the surface of the target material. Differences in erosion behavior are manifested in various mechanisms of material transport, such as tearing and fatigue for rubbers; shear and creep for ductile metals and polymers; crack formation and brittle fracture for ceramics, glass and brittle polymers. Materials are classified as ductile, brittle and semi-ductile according to the dependence of wear rates on impingement angle in the literature. [25].

In this paper, the solid particle erosion behavior of Inconel 718 was studied in detail. When Figure 4 is examined, it is seen that the erosion rate varies significantly depending on the particle impact rate for different particle impingement angles (30, 60, 90). The highest erosion rate was observed at 30° particle impingement angle. The lower erosion rate was followed by 60° and 90° impingement angles, respectively (Fig. 4).

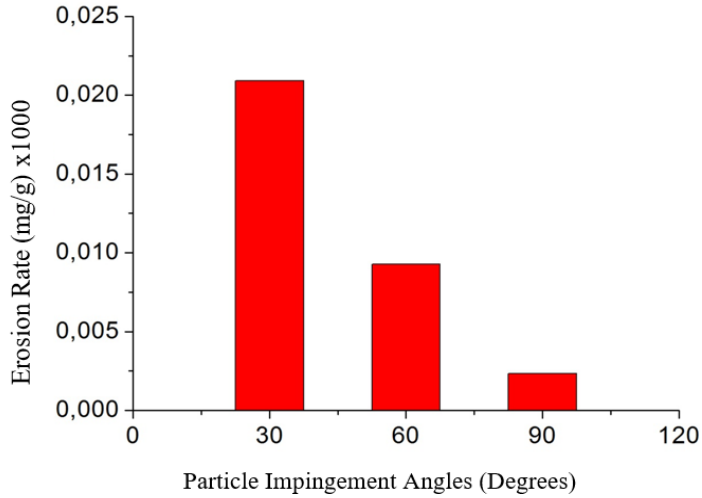

Fig. 4 Change of erosion rates with respect to particle impingement angle

The velocity components of the particles can be divided into horizontal and vertical components. Hard particles, especially when abrading ductile materials, activate the mechanisms of scratching and cutting the material surface with less impact at low impact angles and predominantly horizontal velocity component. As the angle increases, the vertical component of the particle velocity increases and an impact mechanism similar to the impact effect gains weight. With the effect of these mechanisms, it is observed that in ductile materials, when the impact is gradually increased starting from small angles such as approximately 30^{O}, the wear reaches a maximum at moderate impact angles. The sliding and rotation of the particles after contact with the material also leads to different results in the interaction with the material. Ductile and brittle materials show different characteristics when the mass loss in erosion wear is measured as a function of the impingement angle. Ductile materials are characterized by maximum erosion at low impingement angles (15°-30°). Brittle materials show maximum erosion behavior at normal impingement angles (90°). Fiber-reinforced composites show semi-ductile behavior with maximum erosion occurring between 45° and 60° [26].

3.2. Surface roughness and topography investigation

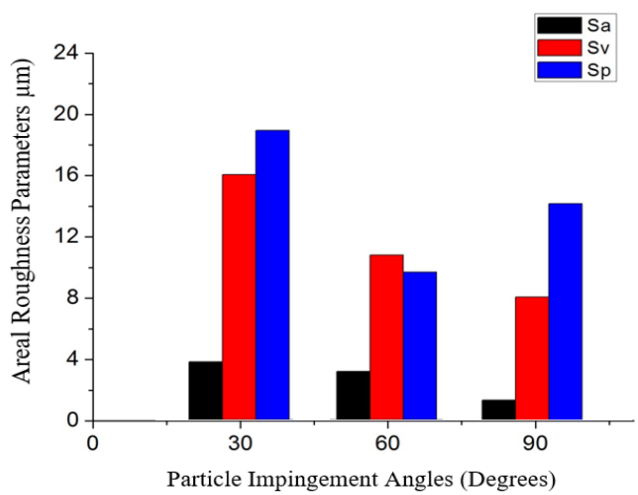

Fig. 5 Change in erosion rates as a function of particle impingement angle

After the solid particle erosion tests, the 3D surface topography and areal surface roughness of the eroded surfaces were determined. Figure 5 shows the graph obtained from the impingement angles of the areal surface parameters of the samples after 30°, 60° and 90°. The maximum wear at 30^{O} impingement angle can be

explained by the fact that more swarf is removed from the specimen surface. This situation also confirms the erosion rate given in figure 4. However, at the 90° impingement angle, no significant increase in the maximum valley height Sv compared to the surface height Sa was observed in Fig. 6c.

As seen in Figure 5, the maximum roughness value occurred in consequence of erosive wear with a particle impingement angle of 30º. In consequence of erosive wear with a particle impingement angle of 90º, it has been observed that very serious pits occur despite the low average roughness value, as well as the minimum erosive wear in the superalloy. The reason for this is that during erosive wear, with a particle impact angle of 90º, the abrasive particles hit perpendicular to the wear surface with high energy [26-30]. Thus, the repetitive impact of abrasive particles on the same points caused an excessive loss of material from that area and caused serious pits to occur. In Figure 6, the variation of the 3D topography of the Inconel 718 superalloy eroded surfaces is given. The amount of erosive wear can be easily read from the ruler given next to the surface topographies, the details of which are shown in different color tones. However, it is possible to see the traces of erosive wear with the 3D topography.

Figure 6.a shows the 3D surface topography of the solid particle eroded coating with a particle impact angle of 30º. In this image, the scale 0 µm represents the deepest part of the eroded coating, and 40 µm the highest part. In other words, erosion occurred at a depth of 40 µm from the surface with solid particle erosion. This erosive wear value of 40 µm is the highest erosive wear value observed in coatings throughout the study. The values obtained from the 3D surface topography confirm the erosion rate and areal roughness values of the previously mentioned pavements. In addition, in Figure 6a, it is seen that the solid particle erosion is eroded in the y direction with a particle impact angle of 30º.

In Figure 6b, the variation of the 3D surface topography of the solid particle eroded pavement with a particle impact angle of 60° is given. Figure 6b shows that solid particle erosion occurs in the y direction with a particle impact angle of 60°. With a particle impact angle of 60°, the solid particle eroded coating suffered an erosive wear of approximately 27.5 µm.

In Figure 6c, the variation of the 3D surface topography of the solid particle eroded pavement with a particle impact angle of 90º is given. As can be easily read from the figure, solid particle erosion with a particle impact angle of 90º resulted in a wear of approximately 20 µm. Therefore, with this wear rate, the particle impact angle at which minimum erosive wear occurs was determined as 90º. It is seen that Inconel 718 superalloy, which undergoes solid particle erosion with a particle impact angle of 90º, exhibits an expected behavior with the previously stated erosion rate and roughness values in the 3D surface topography. As a result, the minimum value was determined at 90º solid particle erosion as a result of the profilometer analyzes obtained in Inconel 718 superalloys, which were exposed to solid particle erosion and erosive wear at 30º, 60º and 90º. This result showed that the Inconel 718 superalloy used in this study exhibited a ductile behavior.

There is a general view that most of the material groups exhibit brittle or ductile behavior as a result of erosive wear. In this case, it generally means that materials subject to solid particle erosion will exhibit brittle or ductile behavior. These two conditions exhibited by the materials emerge as the change in the plastic deformation and erosion rate exhibited by the abrasive particles hitting the surface at different impact angles. General view in the literature; ductile materials have the highest erosion rate at particle impact angles of about 30º and brittle materials at particle impact angles of about 90º [27]. According to the analysis results obtained as a result of Inconel 718 superalloy solid particle erosion, it was observed that they exhibited a ductile behavior.

In the literature, the effect of particle impact angle on the erosive wear behavior of coatings has been investigated in many studies. However, it has been observed that the erosive wear rates are tested gradually at different particle impact angles of 30º, 45º, 60º and 90º [28, 29].

From this point of view, in this study, it has been observed that Inconel 718 superalloy materials, Inconel 718 superalloys, which have been subjected to solid particle erosion at particle impact angles of 30º, 60º and 90º, lose weight in different amounts. Therefore, as a result of exposure of Inconel 718 superalloy abrasive particles at different particle impact angles, each particle exhibited different wear behavior at different impact angles. The highest erosion rate occurred at particle impact angles of 30º, while the lowest erosion rate occurred at particle impact angles of 90º. In other words, the highest amount of wear occurred at particle impact angles of 30º. In addition, it has been reported that as the number of particles hitting the surface increases, the amount of plastic deformation on the coating surface will increase and local delamination occur [31].

According to the results obtained as a result of the change of the three-dimensional surface topography; With a particle impact angle of 30º, the solid particle eroded coating suffered an erosive wear of approximately 40 µm. This erosive wear value of 40 µm is the highest erosive wear value observed in Inconel 718 superalloys throughout the study. This erosive wear value was observed in TBCs that underwent solid particle erosion with wear values of 27.5 µm and 20 µm, respectively, and particle impact angles of 60º and 90º. In this respect, it was seen that the values obtained from the 3D surface topography confirmed the erosion rate and areal roughness values of Inconel 718 superalloys. Likewise, it has been revealed in different studies that these two analysis values confirm each other [21, 31]. Therefore, the ductile behavior of Inconel 718 superalloys has been confirmed once again by the 3D surface topography.

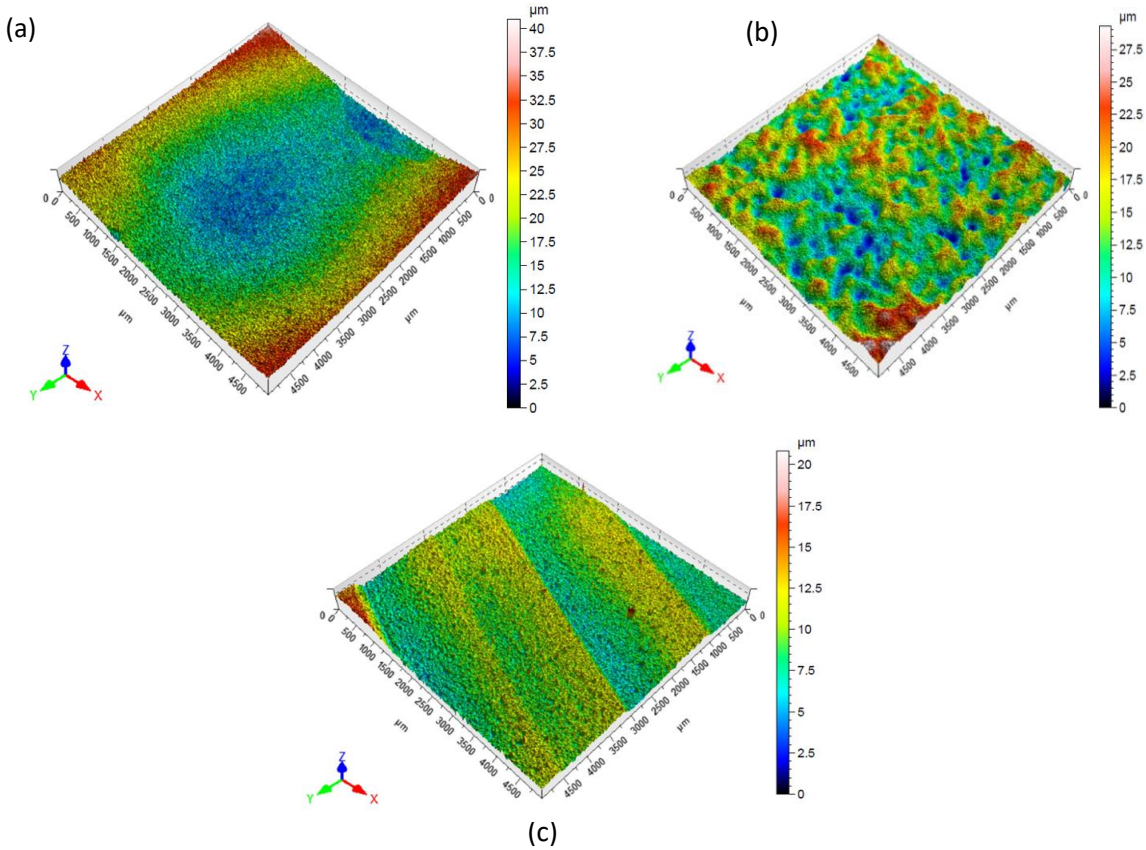

Fig. 6 3D surface topographies of Inconel 718 superalloys eroded (a) 30°, (b) 60° and (c) 90° impingement angles

It has been determined that the main erosive wear mechanisms formed after the erosive wear tests performed at 30º impact angle are micro sliding and micro shearing mechanisms. The fact that these wear mechanisms are effective has led to the formation of valleys and mounds due to both material loss and excessive plastic deformation on the surface. At the 90º particle impact angle, the surface morphology of the Inconel 718 superalloy surfaces has completely changed and the scratches, micro-scratch and micro-cut marks on the surface have completely disappeared. These wear morphologies have been replaced by microcracks and small peaks and pits formed as a result of plastic deformation. These wear mechanisms seen at 90º particle impact angle did not cause an effective material loss on the surface and led to lower mass losses compared to samples abraded at 30º particle impact angle.

4. Conclusion

In this paper, solid particle erosion behavior of Inconel 718 was investigated. Erosion tests were performed at different impact angles (30°, 60° and 90°). The eroded surfaces, erosion rates, areal roughness and surface topography of nickel-based Inconel 718 superalloys were investigated. The major conclusions of the study can be summarized as follows:

- The maximum erosion rates occurred at an impingement angle of 30°.
- It was observed that the highest erosion rate takes placed at the particle impingement angle of 30º, followed by the maximum erosion rate at the particle impact angles of 60º and 90º, respectively.
- It was observed that the surfaces of nickel-based Inconel 718 superalloys used in the tests were significantly affected by the exposure of abrasive particles. The maximum surface roughness was achieved at the 30° impingement angle.
- After 3D surface topography analyzes, it was understood that Inconel 718 superalloys made at particle impact angles of 30º, 60º and 90º were exposed to wear at depths of 40 μm, 27.5 μm and 20 μm, respectively.
- The 3D topographic view of the eroded surfaces openly shows the erosion valleys and damage. The maximum damage occurred at an impingement angle of 30^{O}.
- The erosion mechanisms of Inconel 718 were also shown to vary significantly depending on the impact angle.

Acknowledgements

The experimental studies were supported by Kocaeli University Surface Treatment Laboratory. The author would like to thank Assoc. Prof. Dr. Egemen Avcu from Ford Otosan Ihsaniye Automotive Vocational School, Kocaeli University for their great support throughout the experimental.

References

[1] Zhang, T., Sun, J., & Yuan, H. (2021). Cyclic plasticity modeling and fatigue life assessment of the recasting material of a nickel-based superalloy induced by laser manufacturing. International Journal of Fatigue, 147, 106154.
[2] Cui, H., Tan, Y., Bai, R., Ning, L., You, X., Cui, C., & Li, P. (2023). Deformation and recrystallization behavior of the new Ni-Co based superalloy ingot material prepared by electron beam smelting layered solidification. Journal of Alloys and Compounds, 934, 167880.
[3] Han, C., Zhou, M., Zou, L., Dong, J., Li, Y., Gong, M., & Wang, W. (2023). Effect of flexible machining on subsurface damage and recrystallization of single crystal superalloy. Journal of Manufacturing Processes, 94, 512-523.
[4] Yang, H., Yang, J., Huang, W., Wang, Z., & Zeng, X. (2018). The printability, microstructure, crystallographic features and microhardness of selective laser melted Inconel 718 thin wall. Mater Design, 156, 407-418.
[5] Klotz, T., Miao, HY., Bianchetti, C., Lévesque, M., & Brochu, M. (2018). Analytical fatigue life prediction of shot peened Inconel 718, International Journal of fatigue. 113, 204-221.
[6] Onuiku, B., & Bandyopadhyay, A. (2018). Additive manufacturing of Inconel 718 – Ti6Al4V bimetallic structures, Additive Manufacturing. 22, 844-851.
[7] Desmond, EPK., & Soboyejo, W.O. (2023). Fatigue of Thermostructural Alloys, Comprehensive Structural Integrity. 2, 116-145.
[8] Infante-Garcia, D., Diaz-Alvarez, A., Belda, R., Diaz-Alvarez, J., Cantero, JL., Giner, E., & Miguelez, MH. (2022). Influence of machining parameters on fretting fatigue life of Inconel 718. 162, 106963.
[9] Qi, J., Eri, Q., Kong, B., & Zhang, Y. (2021). The radiative characteristics of Inconel 718 superalloy after thermal oxidation. Journal of Alloys and Compounds, 854, 156414.

[10] Pratheesh Kumar, S., Elangovan, S., Mohanraj, R., & Ramakrishna, J.R. (2021). A review on properties of Inconel 625 and Inconel 718 fabricated using direct energy deposition. Materials Today Proceedings, 46, 7892-7906.
[11] Ćurković, L., Kumić, I., & Grilec, K. (2011). Solid particle erosion behaviour of high purity alumina ceramics. Ceramics International. 37, 29-35.
[12] Oka, YI., Mihara, S., & Yoshida, T. (2009). Impact-angle dependence and estimation of erosion damage to ceramic materials caused by solid particle impact. Wear, 267, 129-135.
[13] Oka, YI., Ohnogi, H., Hosokawa, T., & Matsumura, M. (1997). The impact dependence of erosion damage caused by solid particle impact. Wear. 203, 571-579.
[14] Yildizli, K., Karamis, M., & Nair, F. (2006). Erosion mechanisms of nodular and gray cast irons at different impact angles. Wear. 261, 622-633.
[15] Wang, D., Tian, Z., Shen, L., Liu, Z., & Huang, Y. (2014). Effects of laser remelting on microstructure and solid particle erosion characteristics of ZrO_2–7wt% Y_2O_3 thermal barrier coating prepared by plasma spraying. Ceramics International, 40(6), 8791-8799.
[16] Krishnamurthy, N., Murali, M. S., Venkataraman, B., & Mukunda, P. G. (2012). Characterization and solid particle erosion behavior of plasma sprayed alumina and calcia-stabilized zirconia coatings on Al-6061 substrate. Wear, 274,15-27.
[17] Swain, B., Mallick, P., Gupta, R. K., Mohapatra, S. S., Yasin, G., Nguyen, T. A., & Behera, A. (2021). Mechanical and tribological properties evaluation of plasma-sprayed shape memory alloy coating. Journal of Alloys and Compounds, 863, 158599.
[18] Wang, W., Haché M. J. R., Cheng, C., Lyu, T., Liu, Z., Papini, & M., Zou Y. (2023). Solid particle erosion of a dual-phase $AlCoFeNi_2$ high-entropy alloy. Wear. 528-529.
[19] Nair, R.B., Ngan, & S., McDonald, A. (2023). Dry abrasive wear and solid particle erosion assessments of high entropy alloy coatings fabricated by cold spraying. Materials Today Communications. 34, 105527
[20] Fidan, S., (2014). Tribological performance of polymethyl methacrylate as an aviation polymer. Journal of Polymer Engineering. 34, 569-579.
[21] Patnaik, A., Satapathy, A., Chand, N., Barkoula, N. M., & Biswas, S. (2010). Solid particle erosion wear characteristics of fiber and particulate filled polymer composites: A review. Wear. 268, 249-263.
[22] Infante-Garcia, D., Diaz-Alvarez, A., Belda, R., Diaz-Alvarez, J., Cantero, J. L., Giner, E., & Miguelez, M. H. (2022). Influence of machining parameters on fretting fatigue life of Inconel 718. International Journal of Fatigue, 162, 106963.
[23] TANG, Y., SHEN, X., LIU, Z., QIAO, Y., YANG, L., LU, D., ... & XU, J. (2021). Corrosion behaviors of selective laser melted inconel 718 alloy in NaOH solution. Acta Metall Sin, 58(3), 324-333.
[24] Jones, R., Ang, A., Peng, D., Champagne, V. K., Michelson, A., & Birt, A. (2023). Modelling Crack Growth in Additively Manufactured Inconel 718 and Inconel 625. Metals, 13(7), 1300.
[25] Chowdhury, M.A., Debnath, U. K., Nuruzzaman, D. M., & Islam, M. Experimental analysis of aluminum alloy under solid particle erosion process. Proceedings of the institution of mechanical engineers' part j-journal of engineering tribology. 230, 1516-1541
[26] Arjula, S., Harsha, A. P., & Ghosh, M. K. (2008). Erosive wear of unidirectional carbon fiber reinforced polyetherimide composite. Materials letters, 62(17-18), 3246-3249.
[27] Avcıoğlu, S., Uyan, P., Yontar, O., & Çevik, S. (2022). Electrospray deposition of AlN-PVA composite coating as thermal interface material. Materials Letters, 318, 132235.
[28] Amirthan, G., Udayakumar, A., Prasad, V. B., & Balasubramanian, M. (2010). Solid particle erosion studies on biomorphic Si/SiC ceramic composites. Wear, 268(1-2), 145-152.
[29] Imrek, H., Bagci, M., & Khalfan, O. M. (2011). Solid particle erosion as influenced by tensile axial loads. Tribology transactions, 54(5), 779-783.
[30] Bousser, E., Martinu, L., & Klemberg-Sapieha, J. E. (2014). Solid particle erosion mechanisms of protective coatings for aerospace applications. Surface and Coatings Technology, 257, 165-181.
[31] Kaundal, R. (2017). Role of process variables on solid particle erosion of polymer composites: a critical review. Silicon, 9(2), 223-238.